Original Article

INVESTIGATION OF ANTI-SARS COV-2 ACTIVITY OF SOME TETRAHYDRO CURCUMIN DERIVATIVES: AN *IN SILICO* STUDY

AMRITA MURALIKRISHNAN[a], JASMIN KUBAVAT[a*], MAHESH VASAVA[a*], SRIKANTH JUPUDI[b], NAMITHA BIJU[b]

[a]School of Pharmacy, National Forensic Sciences University, Gandhinagar, Gujarat, India, [b]Department of Pharmaceutical Chemistry, JSS College of Pharmacy, JSS Academy of Higher Education and Research, Ooty, Nilgiris, Tamil Nadu, India
*Email: jasmin.kubavat@nfsu.ac.in

ABSTRACT

Objective: In the current study, an *in silico* approach has been utilized to investigate the anti-SARS CoV 2 activity of some derivatives of Tetrahydro curcumin (THC), a curcumin metabolite.

Methods: BioVia Draw 2017 was used to design 168 THC derivatives. All of the derivatives were docked using Maestro Schrodinger programme. Depending on the docking score, the ADME, drug-likeness, and toxicity prediction of a few THC derivatives were conducted.

Results: 168 THC derivatives were designed. 14 derivatives exhibited a better binding score than Remdesivir. All 14 derivatives' pharmacokinetic characteristics were discovered to be within the acceptable range. Lipinski's rule of five was violated by all derivatives, including the reference drug, yet they all stayed within the recommended range. The greatest docking score among the 14 derivatives was displayed by Structure 21. A study on molecular dynamic (MD) stimulation showed that the protein-ligand complex was relatively stable. Toxicity prediction showed that 14 derivatives were non-hepatotoxic, non-cytotoxic, immunotoxic (except S21), non-mutagenic (except S31) and half of the developed structures were carcinogenic, while the other half, including the standard drug, was non-carcinogenic.

Conclusion: Among 168 THC derivatives, 14 derivatives exhibited better binding score than the reference drug. For all 14 derivatives, pharmacokinetic, drug-likeness, and toxicity prediction were found to be satisfactory. It was discovered that the protein-ligand complex was thermodynamically stable. All 14 compounds present exciting prospects for further *in vitro* and *in vivo* investigation.

Keywords: THC derivatives, Covid-19, SARS CoV 2, Main protease (MPro), Molecular docking

INTRODUCTION

Coronavirus, a virus that has triggered an unending global pandemic, was first discovered in Wuhan city, China, in December 2019 [1]. COVID-19 was declared a pandemic by the World Health Organization (WHO) on March 11 2020 and has been linked to over 50 crores confirmed cases and over 6 million confirmed deaths as of May 2022, making it one of the fatal disease outbreaks in history [2].

Severe Acute Respiratory Syndrome Coronavirus 2 (SARS-CoV-2), a novel beta-coronavirus, is the causative agent for Covid 19 pandemic. They have enveloped viruses with a positive-sense single-stranded RNA genome and a helical symmetry nucleocapsid [3]. The coronaviruses are made up of four structural proteins, namely, the spike (S), membrane (M), envelope (E), and nucleocapsid (N) proteins. Because of the highly conserved nature of Mpro in coronaviruses, this enzyme of SARS-CoV-2 is one of the most appealing antiviral treatment targets [4]. Mopar is the protein of interest since it is involved in processing polyproteins derived from viral RNA. Besides, non-structural proteins (Nsp4-Nsp16), RNA-dependent RNA polymerase (RdRp; also known as Nsp12), and helicase (Nsp13) are considered to rely on Mpro to be cleaved, which is required for virus maturation [5]. Even though vaccines are now available, cases have been reported in people even after two doses of vaccination. Only time will tell how long the vaccine-elicited protection will last and how frequent the booster injections should be administered to keep the protection fully active [6]. Also, since the start of the COVID-19 pandemic, there have been a few significant mutations which have altered the SARS-CoV-2 variants in widespread circulation [7]. For example, the Omicron variant, variant B.1.1.529, was first reported to WHO on 24 November 2021 and was classified as a variant of concern by WHO on 26 November 2021. So, it is possible that further mutations could result in the current vaccines becoming less effective.

Tetrahydro curcumin (THC) is a colourless or white curcumin metabolite initially discovered in 1978 and has been demonstrated to have pharmacological properties similar to curcumin [8]. Tetrahydro curcumin research is becoming more popular as it outperforms Curcumin in water solubility, chemical stability, bioavailability, and anti-oxidative action [9].

The aim of the present study was to identify various tetrahydro curcumin (THC) derivatives as Anti-SARS Cov-2 agents through *in silico* study.

MATERIALS AND METHODS

Designing of ligands

2D structures of 168 THC derivatives were designed using Biovia Discovery Studio 2017. The derivatives were generated by modifying the diketone and two hydroxyl functional groups present in THC (fig. 1).
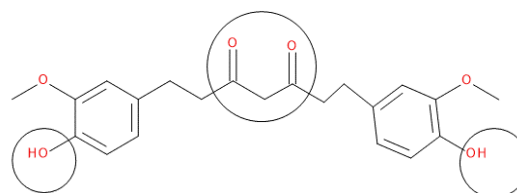
Fig. 1: Design strategy of THC

Ligand preparation

The Ligprep module of Maestro Schrodinger software (Schrödinger Suite, LLC, NY) was used to prepare ligands using the OPLS4 force field.

Prediction of pharmacokinetics and drug-likeness properties

ADMET and drug-likeness properties of 168 THC derivatives were determined using the QikProp module (Maestro 12.8 Schrodinger)

to determine the pharmacokinetic properties of the ligands. The drug-likeness of the designed compounds can be evaluated by considering Lipinski's rule of five or rule of five, which determines whether a compound has physical and chemical properties that would make it an orally active drug in humans [10]. The rule states that a compound should have no more than five hydrogen bond donors, no more than ten hydrogen bond acceptors, a molecular mass less than 500Da and an octanol-water partition coefficient that does not exceed 5.

Protein preparation

The RCSB protein data library was used to obtain the crystal structure of the SARS-CoV-2 Mpro (PDB ID: 5R82). The Protein prepare module (Maestro 12.8 Schrodinger) was used for protein preprocessing, optimization, water removal and energy minimization using the OPLS4 force field.

Receptor grid generation

After protein preparation, the receptor grid was generated using Glide 5.8 (Maestro 12.8 Schrodinger) with default settings for all parameters.

Molecular docking study

Using the computational program Maestro 12.8 Schrodinger, molecular docking studies were conducted to assess the binding energies of THC derivatives to the potential target proteins of SARS-CoV-2. Molecular docking of generated receptor grid and the designed ligands was performed using the Glide extra-standard precision (XP) mode.

MD simulation study

MD simulations were used to evaluate the compound (S21) with the highest scores in complex with the protein Mpro for binding stability and interaction characteristics. MD simulations have been performed with Desmond program, as developed by Schrödinger Materials Science Suite 2021-2. Pressure and temperature were set at 1.0325 bar and 300 K, respectively for 100 nanoseconds and OPLS3e force field was used for energy minimization. NPT ensemble class was used to equilibrate the system. Salt was supplied to the system at particular Na+and Cl charge concentrations: 54.802 mmol (total charge++35) for Na+and 50.105 mmol (total charge-32) for Cl. The MD data were analysed using a number of measures, including Ligand Root Mean Square Deviation, Ligand Root Mean Square Fluctuation, Protein-Ligand interactions, Total Energy, and Ligand Torsion Profile and Properties.

Toxicity prediction

A preliminary review of a compound's harmful characteristics is significant in drug development. Computational toxicity evaluation

has been rapidly advancing as a vital tool for assessing the potential toxicity of chemical structures [11]. The designed structures' toxicity prediction was performed with ProTox II, an online tool for anticipating small molecule toxicity (https://tox-new.charite.de/protox_II/index.php?site=compound_input).

RESULTS AND DISCUSSION

Designing of ligands

By lowering the number of samples needed for *in vitro* and *in vivo* experiments, *in silico* studies could provide useful research data and minimize drug development expenses [12]. The diketone groups were modified into pyrazole rings with various substitutions (R2). Similarly, the two hydroxyl groups were substituted with different groups (R1) (fig. 2). Supplementary material contains the structure of 168 THC derivatives and other related data. (Structure of substituted THC with substitutions represented as R1 and R2).
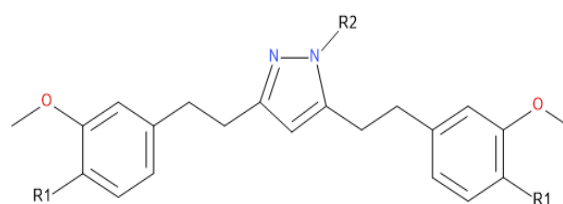
Fig. 2: Structure of substituted THC with substitutions represented as R1 and R2

Prediction of pharmacokinetics and drug likeliness properties

The compounds' pharmacokinetic properties and drug likeness were computed using the Qikprop program (Maestro Schrodinger) and summarized in table 1. For about nine compounds, namely, S7, S8, S9, S10, S14, S25, S26, S27 and S30, the predicted aqueous solubility (QPlogS) was noticed to be beyond the specified range, indicating incomplete solubility of the generated compounds [13]. The permeability of Caco-2 cells, which serve as a model for the gut-blood barrier (QPPCaco), was also high for most of the compounds. The values for brain/blood partition coefficient (QlogBB) and human serum albumin binding (QPlogKhsa) of all 14 compounds and the reference were within the recommended range (−3.0–1.2 and−1.5–1.5, respectively). All derivatives exhibited a significant percentage of human oral absorption. Also, the number of reactive functional groups whose presence can lead to false positives in HTS assays and to decomposition, reactivity, or toxicity problems *in vivo* was found to be 0 for all compounds except for the standard drug, Remdesivir.

Table 1: Predicted ADME pharmacokinetic properties of the best 14 ligands

S. No.	QPlogS (-6.5–0.5)	QPlogHERG (Below-5)	QPPCaco (<25 poor >500 great)	QPlogBB (-3.0–1.2)	QPlogKhsa (-1.5–1.5)	Percent human oral absorption (>80% is high <25% is poor)	No. of reactive functional groups (0-2)
S6	-6.55	-5.467	1049.505	-1.052	1.215	100	0
S7	-8.93	-7.421	833.00	-1.205	1.459	93.827	0
S8	-8.806	-7.396	833.376	-1.213	1.434	100	0
S9	-8.448	-7.395	838.009	-1.26	1.359	100	0
S11	-8.107	-6.444	839.155	-0.962	1.386	100	0
S14	-8.693	-7.432	883.111	-1.372	1.478	100	0
S21	-5.995	-5.49	1374.9	-0.886	1.126	93.276	0
S22	-5.701	-5.614	958.83	-1.07	0.871	100	0
S23	-6	-4.964	1139.422	-0.939	1.221	100	0
S25	-6.915	-5.519	1037.526	-0.849	1.285	92.546	0
S26	-8.646	-8.017	707.542	-1.429	1.579	100	0
S27	-8.582	-7.504	709.886	-1.375	1.356	100	0
S30	-7.622	-6.231	1009.243	-0.859	1.302	100	0
S33	-6	-4.964	1139.422	-0.939	1.221	100	0
Remdesivir	-4.436	-5.862	32.122	-3.082	-0.597	35.213	2

Drug likeness prediction

The ligands' molecular weight, hydrogen bond acceptors, hydrogen bond donors, and octanol-water partition coefficient were calculated to assess drug likeliness, and the results are described in table 2. All 14 derivatives and the reference drug showed at least one violation of Lipinski's rule of five but remained within the suggested range (Maximum is 4).

Table 2: Drug likeness prediction of the best 14 ligands

S. No.	Molecular weight (130.0–725.0)	HB donor (0.0–6.0)	HB acceptors (2.0–20.0)	Qlog Po/w (−2.0–6.5)	Rule of five (Maximum is 4)
S6	458.556	2	4	5.919	1
S7	523.425	2	4	6.921	2
S8	478.974	2	4	6.841	1
S9	462.52	2	4	6.587	1
S11	513.419	2	4	6.817	2
S14	458.556	2	4	6.681	1
S21	444.529	2	4	5.878	1
S22	445.517	2	5	5.182	1
S23	458.556	2	4	5.953	1
S25	523.425	2	4	6.411	2
S26	478.974	2	4	7.168	1
S27	462.52	2	4	6.529	1
S30	496.965	2	4	6.636	1
S33	458.556	2	4	5.953	1
Remdesivir	602.583	5	16.5	1.232	2

Molecular docking

A database of chemical compounds can be rapidly analyzed for possible therapeutic molecules using molecular docking simulations [14]. The 168 THC derivatives and standard drug Remdesivir were docked against the selected target. The docking scores of selected ligands have been summarized in table 3. A negative docking score indicates a strong binding with the target protein, while a less negative or positive score suggests a poor or non-existent binding [15, 16]. The docking study revealed that key sites in Mpro presented great binding affinity with the structures. Structure 21 (S21) had the highest binding affinity with the protein of all the derivatives, which was higher than the reference drug. Thus, this structure may have the most antiviral effect on COVID-19 of all the drugs investigated. The docking score of all 168 derivatives has been included in the supplementary material.

Table 3: Docking scores of the best 14 ligands

S. No.	Docking score	Glide gscore	Glide evdw (Van der waals energy)	Glide ecoul (Coulomb energy)	Glide energy (Modified coulomb-Van der waals energy)
S6	-8.356	-8.356	-49.945	-8.1	-58.045
S7	-8.474	-8.474	-49.451	-7.042	-56.493
S8	-7.919	-7.919	-45.876	-6.588	-52.464
S9	-8.685	-8.663	-47.98	-6.269	-54.248
S11	-8.486	-8.486	-52.334	-7.032	-59.366
S14	-8.301	-8.301	-49.574	-8.288	-57.862
S21	-8.815	-8.815	-43.099	-5.444	-48.543
S22	-8.429	-8.429	-49.389	-7.852	-57.242
S23	-8.359	-8.359	-46.209	-8.19	-54.399
S25	-8.548	-8.548	-47.733	-7.742	-55.475
S26	-8.187	-8.187	-46.946	-9.017	-55.963
S27	-8.663	-8.663	-47.98	-6.269	-54.248
S30	-7.129	-7.129	-47.034	-1.38	-48.414
S33	-8.359	-8.359	-46.209	-8.19	-54.399
Remdesivir	-6.783	-6.783	-48.939	-6.02	-54.959
Native ligand	-5.112	-5.112	-20.73	-4.363	-25.093
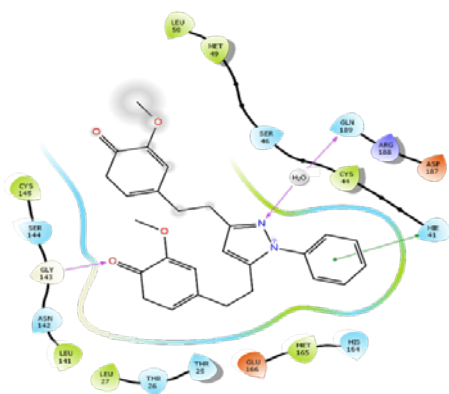
Fig. 3A: 2D interaction diagram of S21 and 5R82
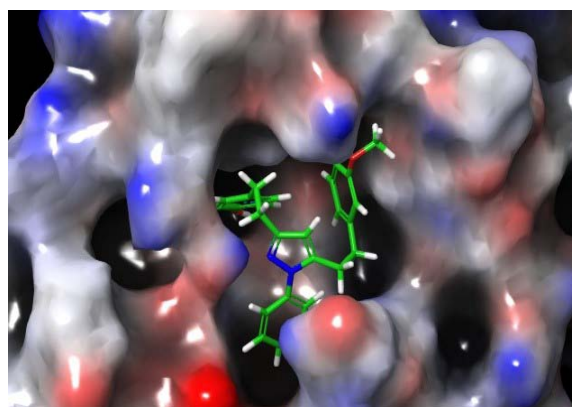
Fig. 3B: Binding of S21 at active site of 5R82

The presence of three hydrogen bonds with GLY143 and the ketone functional group, water molecule and the N atom of the pyrazole moiety, and water molecule and GLN 189 was revealed in fig. 3A, which had the highest docking score. A π-π interaction is observed between the benzene ring attached to the pyrazole moiety and HIE 41. Fig. 3B represents the binding of S21 with active site of 5R82.

MD simulation study

The stability, conformational variations, and underlying molecular interactions of Mpro protein (5R82) at the atomic level was examined using MD simulations at 100 nanoseconds. The specified temperature, pressure, and volume were controlled by simulation quality parameters during the MD simulations [17]. Studies were conducted using various conventional simulation parameters, including Ligand Root Mean Square Fluctuation, Ligand Root Mean Square Deviation, Protein-Ligand interactions, Total Energy, and Ligand Torsion Profile and Properties. Assessing the dynamics and

stability of the protein and its interaction with compound S21 was the primary goal of MD simulation.

The local alterations along the protein chain can be characterised using the Root Mean Square Fluctuation. RMSF of the MPro protein in complex with S21 pattern of residue fluctuations were found to be similar from docked structure of protein ligand shown in fig. 3B and fig. 4A. Throughout the simulation time, proteins showed a rather stable structure without missing any significant interactions. To better comprehend the driving forces behind the stability of protein structure, intramolecular hydrogen bonds were examined. More intramolecular hydrogen bonds are a sign of protein rigidity [18]. In addition to many other characteristics indicated in the figures, the total energy required for stabilising Mpro state in complex with S21 was investigated. A timeline representation of the interactions and contacts shows the total number of specific contacts in which residues interact with the ligand in each trajectory frame as shown in fig. 4B.
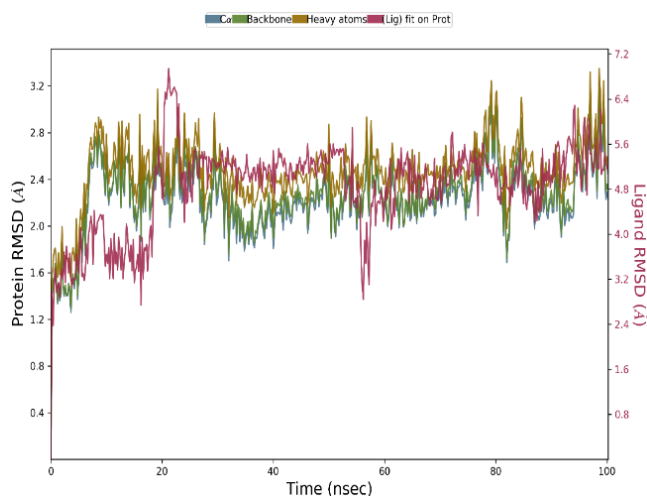
Fig. 4A: Protein ligand RMSD analysis
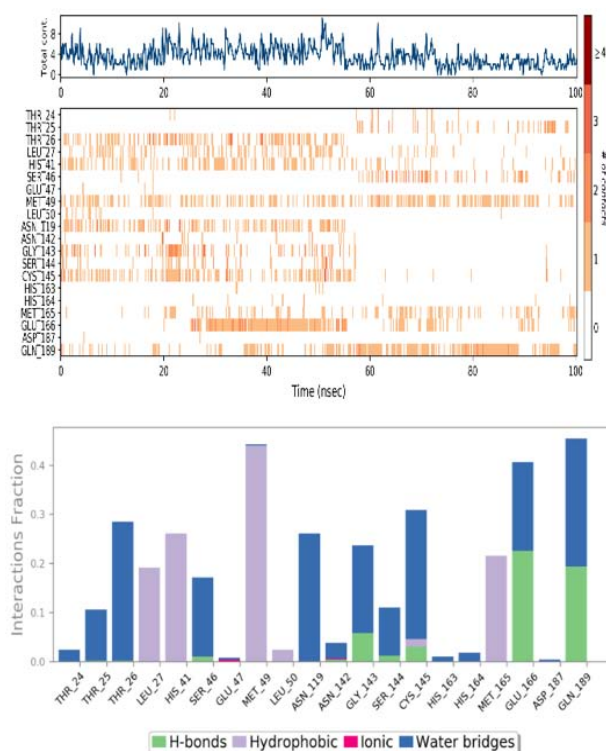
Fig. 4B: Protein ligand contacts

Protein–ligand contact analysis shows that molecule interacts with around 20 active site residues of 5R82 and hydrogen bonds were observed with residues SER46, GLY143, SER144, CYS145, GLU166 and GLN189 as hydrogen-bonding properties is important because of their strong influence on drug specificity, metabolization and adsorption. Compound exhibited hydrophobic interactions with LEU27, HIS41, MET49, LEU50, CYS145 and MET165 as well as a π-π interaction with HIS41. The compound also showed water bridges with THR24, THR25, THR26, SER46, ASN119, ASN142, GLY143, SER144, CYS145, HIS163, HIS164, GLU166, ASP187 and

GLN189. Also, an ionic bond has been observed between the compound and GLU47. Fig. 4C, fig. 4D and fig. 5 shows RMSF analysis of ligand, RMSF analysis of protein and ligand protein contacts respectively.

To comprehend the dynamics associated with it, the torsional degrees of freedom in the ligand provided by rotational bonds were examined. A dial plot and bar plot of the same colour accompany each rotatable bond torsion. In S21, a total of nine rotatable bonds have been identified as illustrated in fig. 6.
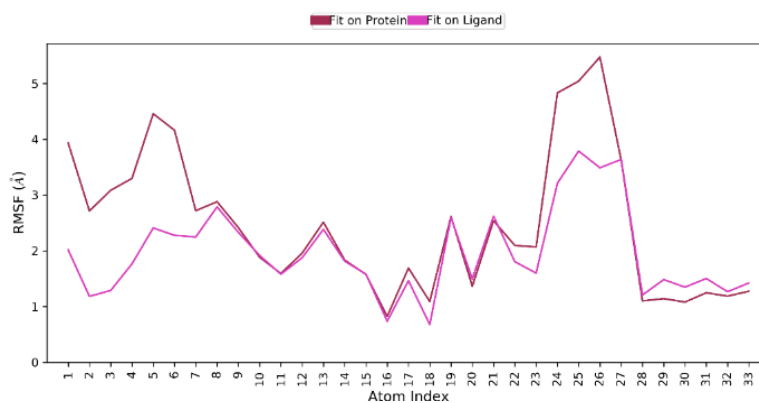
Fig. 4C: RMSF analysis of ligand
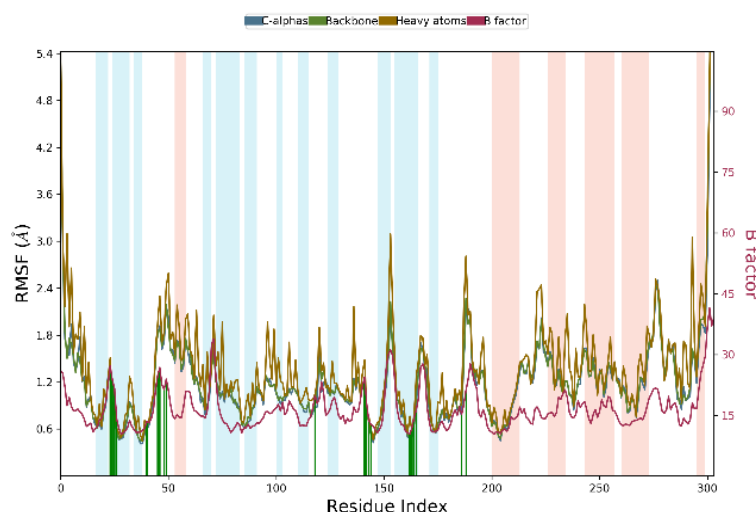
Fig. 4D: RMSF analysis of protein
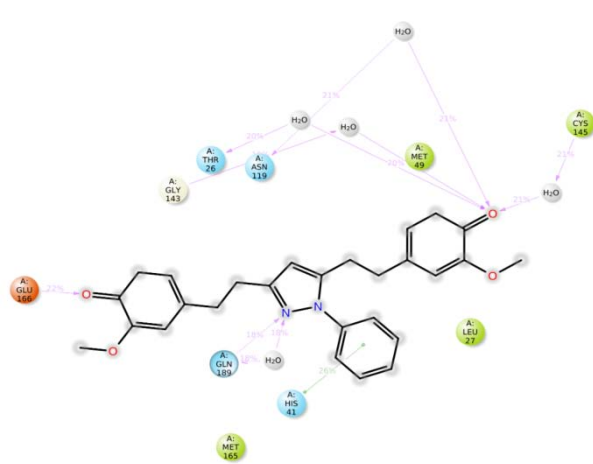
Fig. 5: Ligand protein contacts
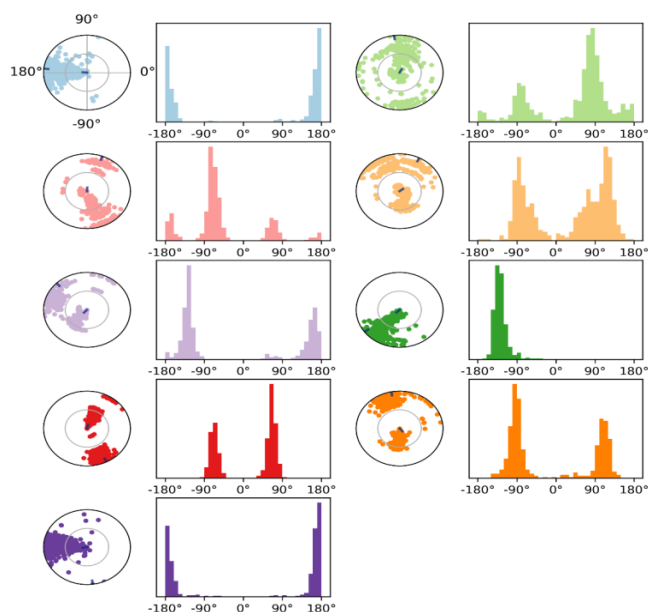
Fig. 6: Ligand torsion profile

Table 4: Toxicity prediction of the best 14 ligands

Compound	H*	P*	CY*	P*	IM*	P*	M*	P*	CA*	P*
S6	I	0.56	I	0.60	A	0.66	I	0.55	A	0.51
S7	A	0.51	I	0.53	A	0.65	I	0.57	I	0.53
S8	I	0.50	I	0.57	A	0.54	I	0.59	I	0.56
S9	A	0.53	I	0.56	A	0.69	I	0.57	I	0.54
S11	I	0.50	I	0.57	A	0.66	I	0.59	I	0.56
S14	A	0.52	I	0.60	A	0.73	I	0.58	A	0.50
S21	I	0.58	I	0.62	I	0.84	I	0.63	A	0.56
S22	I	0.56	I	0.62	A	0.57	I	0.61	A	0.56
S23	I	0.57	I	0.62	A	0.59	I	0.63	A	0.54
S25	I	0.51	I	0.56	A	0.69	I	0.64	A	0.52
S26	I	0.51	I	0.62	A	0.59	I	0.66	I	0.55
S27	A	0.51	I	0.60	A	0.73	I	0.64	I	0.53
S30	A	0.51	I	0.60	A	0.85	I	0.65	I	0.55
S33	I	0.56	I	0.68	A	0.62	A	0.70	A	0.56
Remdesivir	I	0.56	I	0.55	I	0.90	I	0.62	I	0.55

*Where H: Hepatotoxicity, P: Probability, CY: Cytotoxicity, IM: Immunotoxicity, M: Mutagenicity, CA: Carcinogenicity, I: Inactive, A: Active

The compound identified here interact with the Mpro through a variety of non-covalent interactions and hydrogen bonds to engage the same active binding site. The protein and their complex's thermodynamic stability are combined by the current compound under investigation, which is further supported by the computational study.

Toxicity prediction

Organ toxicity and toxicity endpoints

The predicted organ toxicity and toxicity endpoints of the derivatives have been summarized using ProTox II in table 4. Considering the derivatives' organ toxicity (hepatotoxicity), most of them were found to be non-hepatotoxic, including Remdesivir. Most of the molecules were observed to show immunotoxicity except the reference drug. With the exception of S33, which was shown to be mutagenic, all derivatives were found to be non-cytotoxic and non-mutagenic. Regarding carcinogenicity, half of the developed structures were carcinogenic, while the other half, including the standard drug, were non-carcinogenic.

CONCLUSION

The 7th human coronavirus, severe acute respiratory syndrome coronavirus 2 (SARS-CoV-2), was first uncovered in Wuhan, China and has since expanded all across the globe. Precisely, 168 THC derivatives were developed, and the compounds' *in silico* analysis

was performed. Molecular docking studies revealed that the THC derivative with diketone and pyrazole moiety with phenyl group (S21, docking score: -8.815) showed the highest binding energy when docked against 5R82 protein. The estimated ADMET parameters for additional 13 compounds with higher binding energy than the reference medication confirmed that the designed compounds have acceptable pharmacokinetic characteristics. The majority of the derivatives, including Remdesivir, violated at least one rule of five criteria, yet were within the required range, indicating that the compounds could be orally bioavailable. The majority of the compounds were determined to be non-hepatotoxic but caused immunotoxicity. All derivatives were found to be non-cytotoxic and non-mutagenic except S33 for mutagenicity. Considering carcinogenicity, 14 compounds were evenly distributed as carcinogens (S 6, S14, S21, S22, S23, S25, S33) and non-carcinogens (S7, S8, S9, S11, S26, S27, S30. Additionally, MD simulation study was performed to examine the stability and dynamics of the Mpro protein-S21 complex and the results indicated that the docked complex is thermodynamically stable. Further, *in vitro* and *in vivo* research could be conducted to explore the anti-SARS-CoV-2 activity of the above-mentioned compounds.

AUTHORS CONTRIBUTIONS

All the authors have contributed equally.

CONFLICT OF INTERESTS

No potential conflict of interest was reported by the authors.

REFERENCES

1. Mohan BS, Nambiar V. COVID-19: an insight into SARS-CoV-2 pandemic originated at Wuhan City in Hubei Province of China. J Infect Dis Epidemiol. 2020 Jul 18;6(4):146.
2. Cucinotta D, Vanelli M. WHO declares COVID-19 a pandemic. Acta Biomed. 2020 Mar 19;91(1):157-60. doi: 10.23750/abm.v91i1.9397, PMID 32191675.
3. Pal M, Berhanu G, Desalegn C, Kandi V. Severe acute respiratory syndrome coronavirus-2 (SARS-CoV-2): an update. Cureus. 2020 Mar 26;12(3):e7423. doi: 10.7759/cureus.7423, PMID 32337143.
4. Mengist HM, Dilnessa T, Jin T. Structural basis of potential inhibitors targeting SARS-CoV-2 main protease. Front Chem. 2021 Mar 12;9:622898. doi: 10.3389/fchem.2021.622898, PMID 33889562.
5. Naqvi AAT, Fatima K, Mohammad T, Fatima U, Singh IK, Singh A. Insights into SARS-CoV-2 genome, structure, evolution, pathogenesis and therapies: structural genomics approach. Biochim Biophys Acta Mol Basis Dis. 2020 Oct 1;1866(10):165878. doi: 10.1016/j.bbadis.2020.165878, PMID 32544429.
6. Forni G, Mantovani A, COVID-19 commission of accademia nazionale dei lincei, rome. COVID-19 vaccines: where we stand and challenges ahead. Cell Death Differ. 2021 Jan 21;28(2):626-39. doi: 10.1038/s41418-020-00720-9, PMID 33479399.
7. Harvey WT, Carabelli AM, Jackson B, Gupta RK, Thomson EC, Harrison EM. SARS-CoV-2 variants, spike mutations and immune escape. Nat Rev Microbiol. 2021 Jun 1;19(7):409-24.
8. Lai CS, Ho CT, Pan MH. The cancer chemopreventive and therapeutic potential of tetrahydrocurcumin. Biomolecules. 2020 May 29;10(6):831. doi: 10.3390/biom10060831, PMID 32486019.
9. Aggarwal BB, Deb L, Prasad S. Curcumin differs from tetrahydrocurcumin for molecular targets, signaling pathways and cellular responses. Molecules. 2014 Dec 24;20(1):185-205. doi: 10.3390/molecules20010185, PMID 25547723.
10. Chen X, Li H, Tian L, Li Q, Luo J, Zhang Y. Analysis of the physicochemical properties of acaricides based on Lipinski's rule of five. J Comput Biol. 2020 Sep 1;27(9):1397-406. doi: 10.1089/cmb.2019.0323, PMID 32031890.
11. Banerjee P, Eckert AO, Schrey AK, Preissner R. ProTox-II: a web server for the prediction of toxicity of chemicals. Nucleic Acids Res. 2018 Jul 2;46(W1):W257-63. doi: 10.1093/nar/gky318, PMID 29718510.
12. Nazwir N, Yanuar A, Syahdi RR. *In silico* investigation of Echinodermata secondary metabolites as human immunodeficiency virus type 1 (HIV-1) reverse transcriptase inhibitors. Int J App Pharm. 2020 Mar 23;12(1):51-5. doi: 10.22159/ijap.2020.v12s1.FF006.
13. Vasava MS, Bhoi MN, Rathwa SK, Shetty SS, Patel RD, Rajani DP. Novel 1, 4-dihydropyrano [2, 3-c] pyrazole derivatives: synthesis, characterization, biological evaluation and *in silico* study. J Mol Struct. 2019 Apr 5;1181:383-402.
14. Muttaqin FZ, Fakih TM, Muhammad HN. Molecular docking, molecular dynamics, and *in silico* toxicity prediction studies of coumarin, n-oxalylglycine, organoselenium, organosulfur, and pyridine derivatives as histone lysine demethylase inhibitors. Asian J Pharm Clin Res. 2017;10(12):212-5. doi: 10.22159/ajpcr.2017.v10i12.19348.
15. Fan J, Fu A, Zhang L. Progress in molecular docking. Quant Biol. 2019 Jun;7(2):83-9. doi: 10.1007/s40484-019-0172-y.
16. Pagadala NS, Syed K, Tuszynski J. Software for molecular docking: a review. Biophys Rev. 2017 Jan 16;9(2):91-102. doi: 10.1007/s12551-016-0247-1, PMID 28510083.
17. Bhavsar ZA, Acharya PT, Jethava DJ, Patel DB, Vasava MS, Rajani DP. Microwave-assisted synthesis, biological activities, and *in silico* investigation of some benzimidazole derivatives. J Heterocyclic Chem. 2020 Dec;57(12):4215-38. doi: 10.1002/jhet.4129.
18. Vieira DS, Degrève L. An insight into the thermostability of a pair of xylanases: the role of hydrogen bonds. Mol Phys. 2009 Jan 10;107(1):59-69. doi: 10.1080/00268970902717959.